Journal of Physics and Chemistry of Solids 87 (2015) 23–31

Contents lists available at ScienceDirect

Journal of Physics and Chemistry of Solids

journal homepage: www.elsevier.com/locate/jpcs

Enhanced adsorptive removal of Safranine T from aqueous solutions by waste sea buckthorn branch powder modified with dopamine: Kinetics, equilibrium, and thermodynamics

Xiaohui Xu [a,b], Bo Bai [c,*], Honglun Wang [c], Yourui Suo [c]

[a] Shaanxi Key Laboratory of Exploration And Comprehensive Utilization of Mineral Resources, Xi'an 710054, People's Republic of China
[b] College of Environmental Science and Engineering, Chang'an University, Xi'an 710054, People's Republic of China
[c] Northwest Plateau Institute of Biology, Chinese Academy of Sciences, Xining 810001, People's Republic of China

ARTICLE INFO

Article history:
Received 22 April 2015
Received in revised form
30 June 2015
Accepted 29 July 2015
Available online 30 July 2015

Keywords:
Polymers
Chemical synthesis
Surface properties

ABSTRACT

Polydopamine coated sea buckthorn branch powder (PDA@SBP) was facilely synthesized via a one-pot bio-inspired dip-coating approach. The as-synthesized PDA@SBP was characterized using Fourier transform infrared (FTIR) spectroscopy and scanning electron microscopy (SEM). The adsorption progresses of Safranine T on the surface of PDA@SBP adsorbent were systematically investigated. More specifically, the effects of solution pH, contact time, initial concentration and temperature were evaluated, respectively. The experimental results showed the adsorption capacity of PDA@SBP at 293.15 K could reach up to 54.0 mg/g; the adsorption increased by 201.7% compared to that of native SBP (17.9 mg/g). Besides, kinetics studies showed that pseudo-second-order kinetic model adequately described the adsorption behavior. The adsorption experimental data could be fitted well a Freundlich isotherm model. Thermodynamic analyses showed that the ST adsorption was a physisorption endothermic process. Regeneration of the spent PDA@SBP adsorbent was conducted with 0.1 M HCl without significant reduction in adsorption capacity. On the basis of these investigations, it is believed that the PDA@SBP adsorbent could have potential applications in sewage disposal areas because of their considerable adsorption capacities, brilliant regeneration capability, and cost-effective and eco-friendly preparation and use.

1. Introduction

In the past several years, the removal of dyes from industrial wastewater undoubtedly was the hottest topics of discussion, because most dyes are extremely toxic and hazardous to ecosystem and human health [1–4]. To date, various treatment strategies, such as membrane filtration [5], oxidation [6], adsorption [7], electrocoagulation [8], photocatalytic decomposition [9], etc. have been developed and applied in removing dye compounds from wastewater. Among the aforementioned techniques, adsorption is gaining much more popularity owing to its easy operation and high-efficiency [10,11]. Thereinto, using the natural agricultural lignocellulosic byproducts as cheaper and effective biosorbents are gaining public and technological attentions because of their unique merits that were characterized by both environmental conservation and waste recycle. For instance, cotton waste [12], cone shell of calabrian pine [13], coco-peat [14], etc., have been widely utilized to adsorptively remove dyes from wastewater.

Sea buckthorn, as an important economic plant belonging to the family Elaeagnaceae, is one of the most widely distributed economic crops in East Asian. The acreage devoted to sea buckthorn is more than 2.0 million ha in China, accounting for over 90% of the total planting area of the world [15]. As a byproduct of sea buckthorn, sea buckthorn branch (SB), is an abundant bio-resource, which has low utilization at present, mainly as agricultural waste. The chronic and casual management options for these sea buckthorn branches, such as burying them underground, discarding them outside and burning them are characterized by serious resource waste and significant environmental pollution. Therefore, the exploration of finding the effective use of sea buckthorn branches is of particular importance in contemporary society, because waste sea buckthorn branches still have various primitive advantages including that they are very inexpensive, completely biodegradable, incredibly abundant, and clearly renewable.

The chief chemical constituent of sea buckthorn branch is cellulose, hemicellulose, and lignin. There are various inherent reactive functional groups, such as hydroxyl, carboxyl, ether,

* Corresponding author. Fax: +86 29 82339961.
E-mail address: baibochina@163.com (B. Bai).

http://dx.doi.org/10.1016/j.jpcs.2015.07.022
0022-3697/

phosphate, and amino groups on the surface of sea buckthorn branch [16]. The existence of these functional groups endows the raw SBP with talent adsorption ability for organic dyes or metals ion through covalent and non-covalent interactions. Nevertheless, compared with normal absorbents with special porous structure or functionalizated surface, the native form of SBP usually lack high adsorption capacity and efficiency because of their low-level adsorption active sites and low density of active anchoring sites per unit surface area. To enhance their adsorption ability and efficiency, surface functionalization or modification of SBP via a facile, green method is urgently needed, but remains challenging. Dopamine, a long-lasting adhesive protein secreted by mussels, can undergo self-polymerization when dipped into alkaline or oxidants contained aqueous solutions, and the resultant polydopamine (PDA) containing numerous catechol groups, amine groups and aromatic rings [17]. Taking into consideration the existence of such abundant reactive groups, polydopamine is expected to offer a large number of active sites for binding heavy metal ions or organic pollutants through electrostatic, bidentate chelating, or hydrogen bonding interactions [18], which has stimulated extensive researches on the polydopamine-based adsorbent materials. Typically, Fu et al., have demonstrated that PDA microspheres could serve as a high-efficiency adsorbent for the removal of methylene blue from aqueous solutions [19]. Farnad's groups have directed the use of polydopamine nanoparticles as an adsorbent for copper ions from wastewater [20]. However, significant limitations, including the very high-cost of dopamine material and the ineffective use of the interior of polydopamine microspheres hinder their commercialization and industrialization on a large scale.

As stimulated by this background, in the present study, a simple but versatile strategy of preparing polydopamine coated sea buckthorn branch powder (PDA@SBP) biosorbent for dye removal was proposed, i.e., encapsulating individual SBP with functionalizable, artificial organic polydopamine shells through strong covalent bonds was carried out. Safranine T, as a typical dye of organic compound used in industry was chosen to be studied over a batch adsorption system. The removal of Safranine T from aqueous solution using PDA@SBP as adsorbent was systematically investigated. Experiments were carried out to evaluate the effect of solution pH values, contact time, and initial dye concentration on the removal of Safranine T. The sorption kinetic and isotherm models of adsorption process, and the regeneration of the spent PDA@SBP adsorbent were also investigated. In generally, the surface modification of SBP with dopamine not only have extended the utilization of waste sea buckthorn branches and avoided unnecessary dopamine consuming, but also enhanced dye adsorption capacity due to an increase of surface active anchoring sites. Besides the advantage of using abundant, non-toxic and low-cost natural resources, the modification method has simplified the synthetic route greatly.

2. Experimental

2.1. Materials

Sea buckthorn branch (SB) was collected from countryside (Qinghai, China). Dopamine hydrochloride and tris(hydroxymethyl)aminomethane (Tris–HCl) were supplied by Tianjin Chemical Reagent Factory (Tianjin, China). Safranine T (ST) was supplied by Beijing Oriental Chemical Factory (Beijing, China). The chemical structure is depicted in Scheme 1. All the chemicals used in the present study were of reagent grade and were used without further purification.

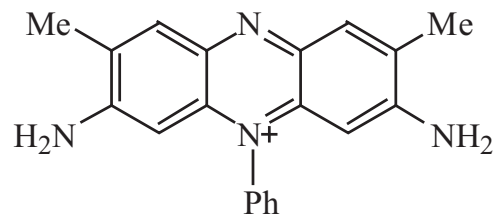

Scheme 1. Structure of safranine T dye.

2.2. Preparation of PDA@SBP adsorbent

Raw waste sea buckthorn branches were cleaned, dried and pulverized in a crushing machine. The neat SBP was dipped into a dilute aqueous solution of dopamine (2 mg/mL), buffered to alkaline conditions using a mixed solvent of Tris–HCl buffer solution (10 mM, pH 8.5). The mixture was stirred gently for 4 h at room temperature. After the reaction, the products were centrifuged, washed with distilled water and dried to yield PDA@SBP.

2.3. Characterizations of PDA@SBP samples

The functional groups of the obtained PDA@SBP were confirmed using a Perkin Elmer FTIR System 2000 in 400–4000 cm^{-1} range via KBr pellet. A Hitachi S-4800 scanning electron microscope was used to observe the surface morphology of PDA@SBP. Shimadzu-18A UV–visible spectrophotometer was employed to measure the dye concentration.

2.4. Adsorption studies

The dye adsorption studies were carried out using batch method. In brief, 0.05 g of dried adsorbent was soaked in 25 mL of dye solution. The beakers containing adsorbent and dye solutions should be protected from light in a dry place. At different time intervals, about 2.0 mL of dye solution was removed and measured using UV–visible spectrophotometer to determine the dye concentration. The amount of adsorbed dye q_t (mg/g) at various times (t) and at equilibrium q_e (mg/g) and removal efficiency (R %) was calculated using following relations:

$$q_t = \frac{(C_0 - C_t)\cdot V}{m} \tag{1}$$

$$q_e = \frac{(C_0 - C_e)\cdot V}{m} \tag{2}$$

$$R\% = \frac{(C_0 - C_e)}{C_0} \times 100 \tag{3}$$

where C_0 is the initial dye concentration, C_t and C_e are concentration at time t and at equilibrium of the dye (mg/L), respectively. V (L) is the volume of dye solution and m (g) represents the weight of the dry absorbent. All the experiments were performed in triplicates to minimize error and the results were averaged.

2.5. Desorption and reusability

0.05 g of PDA@SBP loaded with ST was soaked in 50 mL of various desorbing mediums, including distilled water, HCl (0.1 M) and CH_3COOH (0.1 M) for a period of 2.0 h. The amount of ST desorbed was measured spectrophotometrically and calculated using equation below

$$\text{Amount of ST desorbed}(\%) = \frac{W_d}{W_a} \times 100\% \quad (4)$$

where W_d (mg/g) is the amount of ST desorbed by reagents, W_a (mg/g) is the amount of ST adsorbed onto PDA@SBP. After desorption, the PDA@SBP was contacted again with dye solution for another cycle of adsorption and then treated with 0.1 M HCl for another desorption cycle. The adsorption–desorption procedures were repeated five times to confirm the reusability of the PDA@SBP absorbent.

3. Results and discussion

3.1. Synthesis and characterization of PDA@SBP absorbent

Possible deposition process of PDA on the surface of SBP substrate and subsequent adsorption of ST are schematically illustrated in Scheme 2.

The inherent reactive functional groups on the external surface of SBP, such as hydroxyls and carboxyls, are able to capture dopamine molecules in an aqueous dopamine (dopamine hydrochloride) solution [21]. According to previous reports [22], dopamine is easily oxidized and self-polymerized in weak base conditions and consequently adhered to the surface of various substrates in the form of a PDA shell. As depicted in Scheme 2, dopamine is first oxidized and cyclized to dopaminechrome followed by rearrangement to yield 5,6-dihydroxyindole. Thereafter, 5,6-dihydroxyindole further suffers from polymerization to form polydopamine, leading to the formation of a thin polydopamine precipitate [23].

Thus, in the current work, when SBP substrate was immersed into an aqueous dopamine (dopamine hydrochloride) solution buffered to pH=8.5, covalent and non-covalent interactions including the hydrogen bond, π–π interactions, and electrostatic interactions between dopamine and the SBP substrate were built up [24], making a PDA layer that was tightly and uniformly stuck to the surface of the SBP substrate (denoted here as PDA@SBP). This procedure was confirmed during the synthesis by a visible alteration of the color of the dopamine solution from pale brown to dark when the PDA shell was successfully created on the surface of the SBP host. Obviously, plenty of phenolic functional groups as well as aromatic rings were introduced onto the SBP surface. These groups are of great importance because the numerous catechol groups, amine groups and aromatic rings could afford active sites for binding ST molecules onto the surface of PDA@SBP from aqueous solutions via electrostatic interaction, hydrogen bonding or π–π stacking interactions [19,25]. By this mean, the adsorption capability of PDA@SBP could be greatly improved in comparison with the naked SBP substrate.

From the above analysis, it can be supposed that the pristine SBP and dopamine play their own extraordinarily important roles simultaneously. On one hand, the substantial functional groups on the surface of SBP provide an outstanding ability to capture dopamine molecules firstly. Such fixation functions of dopamine molecules make the grafted self-polymerization reaction of PDA occur on the SBP surface inevitably. On the other hand, the coarse surface of SBP substrate provides an excellent platform for the dispersion of PDA, which will contribute to the adsorption of ST molecules because of the increased quantity of adsorption site. Similarly, the polydopamine shell uniformly coated on the SBP substrates can offer a large number of active sites for binding ST molecules owing to the strong affinity between the aromatic rings of polydopamine and ST molecules. In brief, compared with the pure PDA microspheres, the internal polydopamine of PDA microspheres is partially replaced by cheap SBP, avoiding unnecessary waste of expensive dopamine resources. At the same time, the high-level adsorption ability of polydopamine is persisted, and the mechanical stability of the fragile PDA copolymer is strengthened because the SBP substrates have considerable tensile strength. From this point of view, the obtained PDA@SBP composite is demonstrated to be a new dye absorbent with low cost, considerable adsorption capacity, simple preparation, and practical applicability.

To verify the successfully synthesized PDA@SBP, Fourier transform infrared (FTIR) spectroscopy was employed to characterize the structures of the intermediates and the final products. The FTIR spectra of the powdered sea buckthorn branches, dopamine, PDA and PDA@SBP are presented in Fig. 1.

In Fig. 1, the absorption band near 3458 and 2924 cm^{-1} in the spectrum of SBP (Fig. 1(c)) were ascribed to the stretching vibrations of the hydroxyl group (–OH) and C–H of the methylene group, respectively. The wave numbers at 1113 cm^{-1} and 880 cm^{-1} were due to ring vibrations of glycosidic bonds [26]. The above peaks were assigned to the characteristic absorption bands of the cellulose structures. The peaks at 1640 and 1400 cm^{-1} were ascribed to the stretching vibrations of the skeletal C=C in the aromatic rings bands of lignin [27]. In the spectra of dopamine (Fig. 1(a)), many narrow and sharp absorption peaks can be observed, a characteristic of small molecules. In the spectrum of the PDA (Fig. 1(b)), the broad band at 3458 cm^{-1} was assigned to the stretching O–H/N–H bonds, and the bands appearing at 1642 and 1400 cm^{-1} were related to the overlap of C=C resonance vibrations in the aromatic ring and phenolic C–O–H stretching vibration at 1300 cm^{-1} [28]. The features of the absorption bands of dopamine and PDA imply the successful oxidation polymerization of dopamine. Compared with the spectrum of naked SBP, a more intense peak at 1400 cm^{-1} and a new peak at 1300 cm^{-1} were

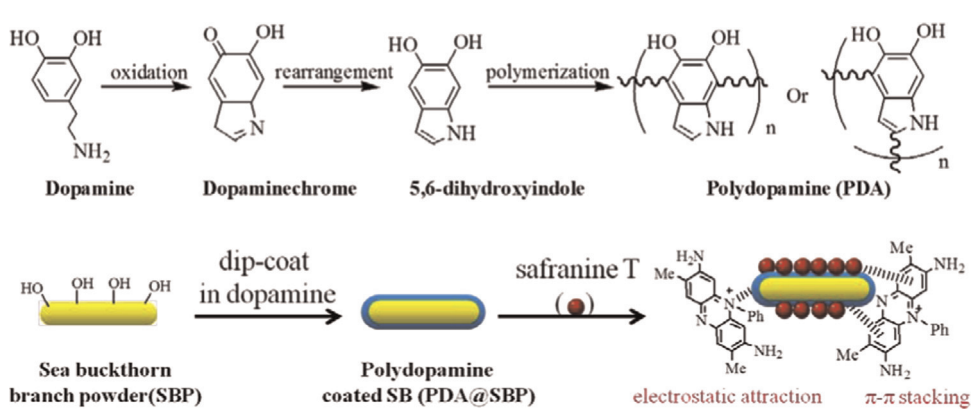

Scheme 2. Schematic illustration of the deposition process of PDA on the SBP surface and subsequent interactions between the PDA@SBP and ST.

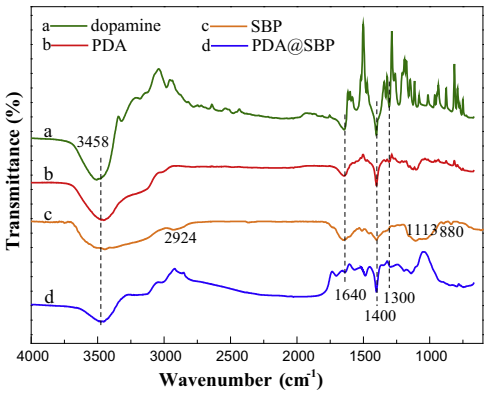

Fig. 1. FTIR spectra of dopamine, PDA, SBP and PDA@SBP.

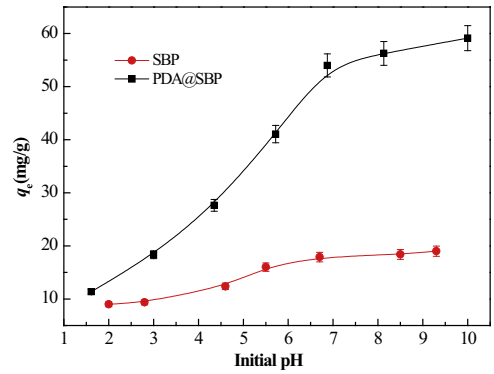

Fig. 3. Effect of initial pH on the adsorption of ST onto the PDA@SBP and SBP. Conditions: dye concentration: 100.0 mg/L; mass of adsorbent: 50.0 mg; temperature: 293.15 K.

obtained in the spectrum of PDA@SBP, suggesting the presence of polydopamine on the surface of SBP.

The coating of PDA active layer on the surface of virgin SBP scaffold can be further verified by their SEM images. In this regard, the surface topographies of the primitive SBP substrate and the PDA@SBP were visualized by SEM with high-resolution and the images are displayed in Fig. 2. It can be observed that the native SBP has a relatively smooth surface structure, while the PDA@SBP possesses a rough surface with numerous microsized aggregates and folds. The change of surface morphology is due to the accumulation and coalition of the PDA layer on the surface of the neat SBP substrate. Brunauer–Emmett–Teller (BET) surface areas of SBP (c) and PDA@SBP (d) were calculated from nitrogen adsorption isotherms (Fig. 2c and d). The BET surface area of SBP is 8.60 m^2/g and PDA@SBP is 7.49 m^2/g, respectively. In addition, the pore volume has also decreased from 0.02 cm^3/g to 0.01 cm^3/g. It is obvious that the BET surface areas of PDA@SBP have been decreased and a few pore canals pure SBP have been blocked, demonstrating again the successful deposition of a PDA layer onto the surface of SBP substrate.

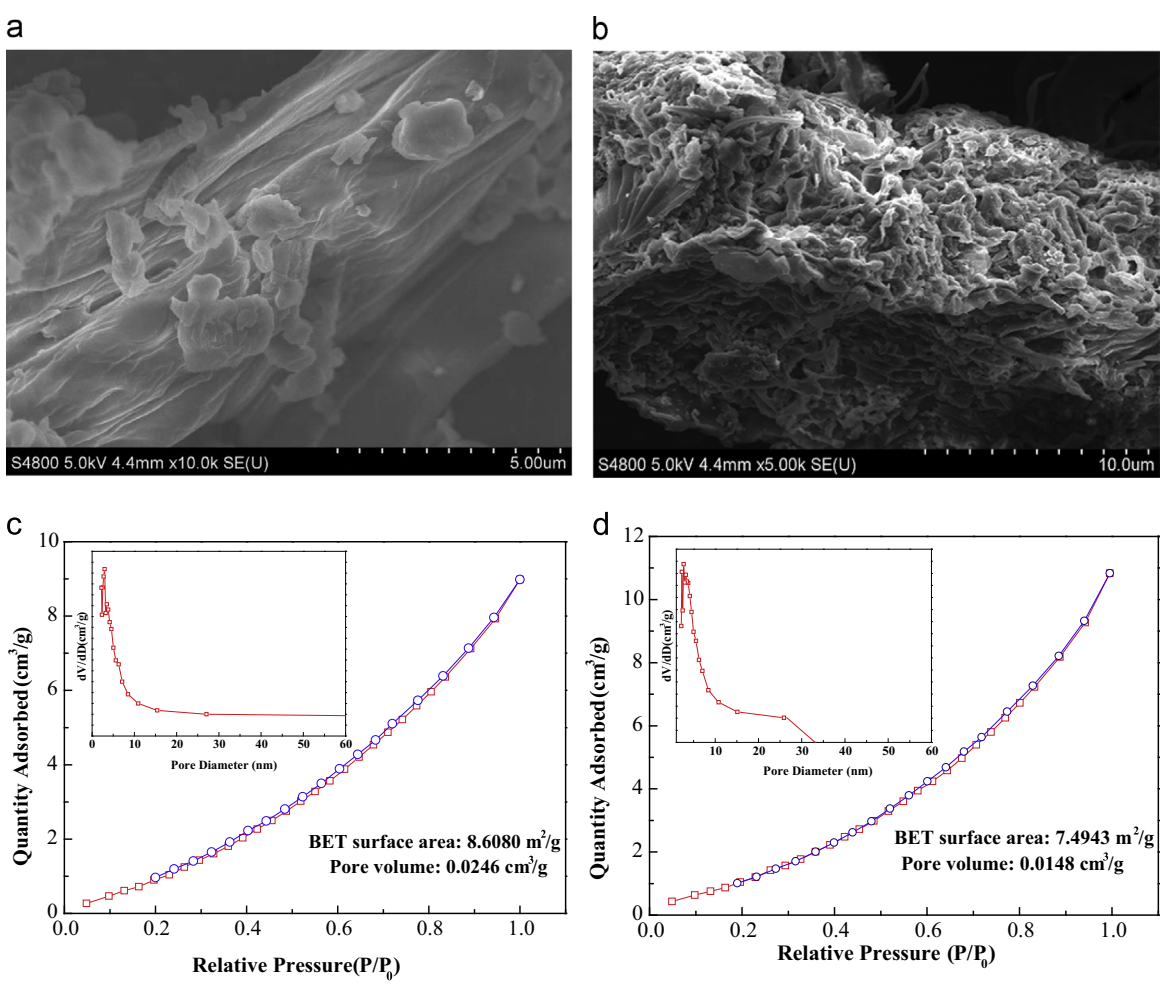

Fig. 2. SEM micrographs of primitive SBP (a), PDA@SBP (b); nitrogen adsorption/desorption isotherms and pore size distribution (inset) of SBP (c), PDA@SBP (d).

3.2. Dye uptake study

3.2.1. Effect of initial solution pH on dye adsorption

The level of acidity or alkalinity of an adsorption medium, which could have an impact on the degree of speciation of adsorbate, is one of the most significant factors influencing the whole adsorption process. Thus, the effects of initial solution pH on the adsorption capacity of the ST dye for a feed concentration of 100.0 mg/L in the pH range of 1.0–10.0 were studied as shown in Fig. 3. With the increasing of pH from 1.6 to 10.0, the sorption capacities of PDA@SBP and native SBP toward ST both present an increasing trend. And the PDA@SBP adsorbed up to 94.62% of ST while the removal efficiency of the pure SBP without dopamine modification was only 28.84% for the initial pH of 10.0. The enhanced adsorption capacity of the PDA@SBP may be attributed to existence of active quinone groups generated by oxidation of free catechols in the polydopamine coating, which provide some additional adsorption sites to effectively bind ST molecules [29,30]. It indicates that PDA@SBP composite can act as a highly effective adsorbent for ST molecules sorption after dopamine treatment and basic solutions are conducive to dye adsorption. Hence, the initial pH has played an important role in the adsorption capacity of ST. The reason may be largely attributed to the surface charge change of PDA@SBP [31]. More specifically, at strongly acidic condition (pH < 3.0), most of the amino functional groups of the PDA@SBP are protonated, i.e., the PDA@SBP is positively-charged and then interacts with the cationic dye molecules via electrostatic repulsion force, leading to the reduction of the adsorption capacity. However, when pH is 3.0, the adsorption amounts of ST can still reach 18.35 mg/g. This may be ascribed to the mutual effects between dye molecules and PDA@SBP, i.e., the π–π stacking interactions between the aromatic rings of polydopamine layer and dye molecules as well as the hydrogen bond reciprocities between the catecol moieties of PDA and functional groups of adsorbate [32]. At higher pH values (pH > 3.0), the deprotonation of the phenolic functional groups of PDA@SBP occurs, the surface charge of the adsorbent become negative. So, the amount of ST dye adsorption tends larger. The larger sorption capacity of PDA@SBP reveals that the introduction of PDA coating onto raw SBP material can significantly improve the sorption performance.

3.2.2. Effect of contact time and adsorption kinetics

The kinetics of dye adsorption can be depicted by the acquisition of adsorbate molecules which defined the residence time needed for the completion of adsorption process. The effect of contact time on dye adsorption onto PDA@SBP is shown in Fig. 4. As can be seen, initially ST dye adsorption on the surface of PDA@SB is a rapid process, followed by a much slower second step till it reaches the equilibrium condition and no further increase in the adsorbing capacity. The tendency of ST dye adsorption may be due to the availability of functional groups of PDA@SBP in ample quantities, and gradual consumption of these reaction sites. And the adsorption capacity at equilibrium of PDA@SBP for the concentration of 100 mg/L can reach up to 54.0 mg/g which is larger than that of the virgin SBP substrate (17.9 mg/g). However, the time to be equilibrium was observed to be independent of feed concentration of ST dye.

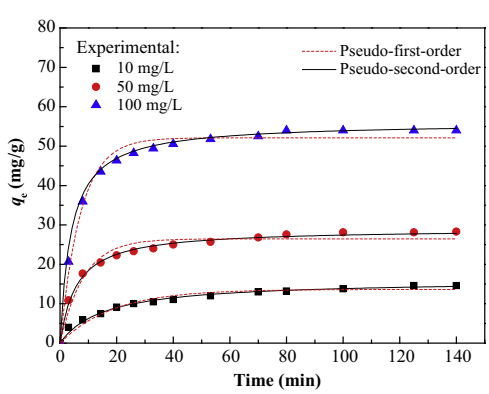

Fig. 4. Time-course profiles of adsorption of ST onto PDA@SBP at different initial concentrations: pseudo-first- and pseudo-second-order kinetic models. Conditions: mass of adsorbent: 50.0 mg; pH: 6.8; temperature: 293.15 K.

For further evaluating the potential adsorption determining steps involved in the ST adsorption process, the experimental data were fitted to the following pseudo first-order equation (Eq. (5)) of Lagergren and pseudo second-order formula (Eq. (6)) of Ho and Mckay as also shown in Fig. 4 with solid and dotted lines, respectively

$$\text{Pseudo–first – order:} \qquad q_t = q_e\left(1 - e^{-K_1 \cdot t}\right) \tag{5}$$

$$\text{Pseudo – second – order:} \qquad q_t = \frac{K_2 \cdot q_e^2 \cdot t}{1 + K_2 \cdot q_e \cdot t} \tag{6}$$

where q_e and q_t (mg/g) represent the amount of dye adsorbed on PDA@SBP at equilibrium and time t (min), respectively; K_1(min^{-1}) and K_2 (g/mg min) are the kinetic rate constants of the pseudo 1st order and pseudo 2nd order models, respectively.

The parameters and coefficients for the two kinetic models were determined by nonlinear fitting technique, and the kinetic parameters are summarized in Table 1. From Fig. 4 and the obtained correlation coefficients (R^2) of Table 1, it is evident that the adsorption of ST over PDA@SBP can be characterized by a pseudo 2nd order kinetic model in the present study. This result suggests that the rate-controlling step may be a chemical adsorption including valence forces by ion exchange between the ST dye and adsorbent [33], i.e., the adsorption process is controlled by the chemical interaction between the ST and PDA@SBP surfaces.

With the aim to gain more insight into the kinetics of adsorption process, intraparticle diffusion and Elovich kinetic models were applied. The Elovich equation in linear form can be represented as [34]

$$q_t = \frac{1}{\beta}\ln(\alpha\beta) + \frac{1}{\beta}\ln(t) \tag{7}$$

where α (mg/g min) is related to the initial adsorption rate and the parameter β (g/mg) is related to the extent of surface coverage and activation energy for chemisorption. Plot of q_t versus ln$t$ (Fig. 5a) lead to a straight line that the Elovich parameters obtained from its slope and intercept respective recent are reported in Table 2. Values of α and β changed as a function of the initial dye concentrations. Also, the experimental data give a good correlation for these results. It is obvious that adaptability of the Elovich equation for the experimental kinetic data suggests that the Elovich model was unable to describe properly the kinetics of the ST dye on the PDA@SBP adsorbents.

Intraparticle diffusion model based on the theory proposed by Weber and Morris is represented by the famous wellknown equation [35]

$$q_t = k_{id} t^{0.5} + C \tag{8}$$

where k_{id} (mg/g min$^{0.5}$) is the intraparticle diffusion rate constant and constant C (mg/g) is the intercept. Values of k_{id} and C were calculated from the slope of linear plot of q_t versus $t^{0.5}$ (Fig. 5b) and the results are listed in Table 2. In the present study, the regression of q_t versus $t^{0.5}$ is linear, but the plots do not pass through the origin. This phenomenon indicates that adsorption involved intraparticle diffusion, but that is not the only controlling factor in

Table 1
The kinetic parameters and coefficients of the pseudo-first-order and the pseudo-second-order model for ST adsorption onto PDA@SBP.

C_0 (mg/L)	Pseudo-first-order					Pseudo-second-order			
	$q_{e,exp}$ (mg/g)	K_1 (min^{-1})	$q_{e,calc}$ (mg/g)	R^2	χ^2	K_2 (g/mg min) × 10^{-3}	$q_{e,calc}$ (mg/g)	R^2	χ^2
10	5.9	0.053	13.63	0.9552	0.8305	5.17	15.6	0.9897	1.071
50	28.3	0.120	26.46	0.9549	2.85964	6.38	29.2	0.9982	0.052
100	54.0	0.138	52.10	0.9357	71.225	5.05	55.5	0.9992	0.006

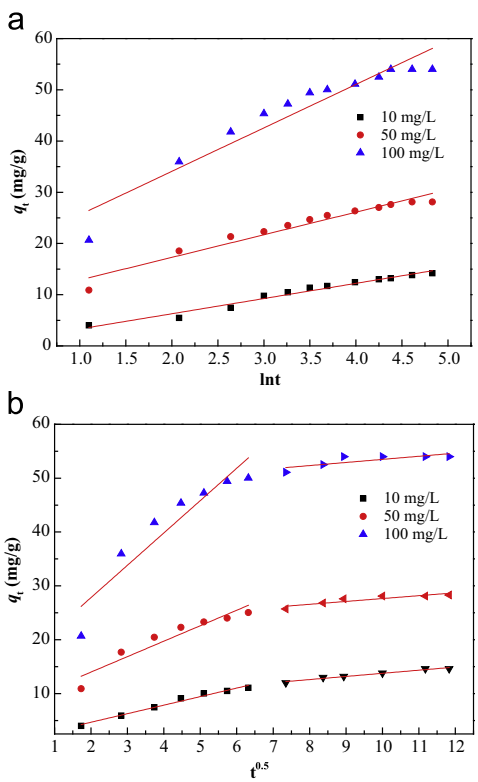

Fig. 5. (a) Elovich kinetic model and (b) intraparticle diffusion plots for ST adsorption. Conditions: mass of adsorbent: 50.0 mg; pH: 6.8; temperature: 293.15 K.

determining the kinetics of the process [36]. The C values (7.955 mg/g) increased with the initial dye concentrations (10–100 mg/L), implying that increasing the initial ST concentrations promotes the boundary layer diffusion effect.

3.2.3. Effect of initial concentration and adsorption isotherms

The effects of initial dye concentrations on the rate of adsorption and removal efficiency of ST dye onto PDA@SBP were investigated between 10.0 and 120.0 mg/L at solution pH of 6.8. As can be noticed from Fig. 6, the PDA@SBP exhibited high adsorption capacity and removal efficiency of the ST dye. The enhanced adsorption capability or high removal efficiency is mainly caused by the strong electrostatic attraction among surface functional groups of the adsorbent with the cationic dye molecules. It can also be noticed that,

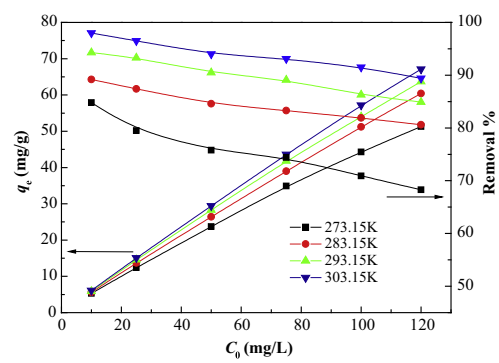

Fig. 6. Effect of feed concentration (10.0–120.0 mg/L) on dye adsorption at different temperatures. Conditions: mass of adsorbent: 50.0 mg; pH: 6.8.

as feed concentration changed from 10.0 to 120.0 mg/L, adsorption of PDA@SBP greatly increased while the removal efficiency decreased clearly at all temperature. Because the total ST adsorption capability is fixed, the quantity of unabsorbed ST in the solution is also high at higher initial dye concentration, resulting in the sustained downward trend of the removal efficiency [37]. In addition, the saturated reaction sites of the PDA@SBP could also contribute to the gradual decrease in the removal efficiency [38].

The isotherms of adsorption are one of the most important characteristics in describing the interaction between the molecules of ST dye and adsorbent surface sites and also, in optimizing the utilization of adsorbent. Here, several commonly employed models were developed to test the experimental data, including two-parameter Langmuir and Freundlich isotherm models. The Langmuir isotherm presumes that adsorption occurs at particular homogenous sites within the adsorbent, where the sorption of each sorbate molecule onto adsorbent surface has uniform sorption activation energy. The Freundlich model is an empirical equation used to depict heterogeneous and multilayer adsorption, and the heterogeneity is caused by the existence of various functional groups over the adsorbent surface and also by the different interaction mechanisms between adsorbate and adsorbent [39].

The linearized form of the models can be expressed by the following equations:

$$\text{Langmuir isotherm:}\quad \frac{C_e}{q_e} = \frac{1}{q_{max}.K_L} + \frac{C_e}{q_{max}} \tag{9}$$

$$\text{Freundlich isotherm:}\quad \ln q_e = \frac{1}{n}\cdot \ln C_e + \ln K_F \tag{10}$$

Table 2
Elovich and intraparticle diffusion parameters at different initial concentrations.

C_0 (mg/L)	Elovich model				Intraparticle diffusion model				
	α (mg/g)	β (mg/g min)	R^2	χ^2	$K_{id,1}$ (mg/g min$^{1/2}$)	$K_{id,2}$ (mg/g min$^{1/2}$)	C (mg/g)	R^2	χ^2
10	3.145	0.338	0.9709	0.9312	1.586	0.5804	7.955	0.9768	0.158
50	25.50	0.222	0.9457	0.8869	2.870	0.5343	22.30	0.8895	2.658
100	63.77	0.118	0.9105	8.5414	6.006	0.5753	47.74	0.8609	15.02

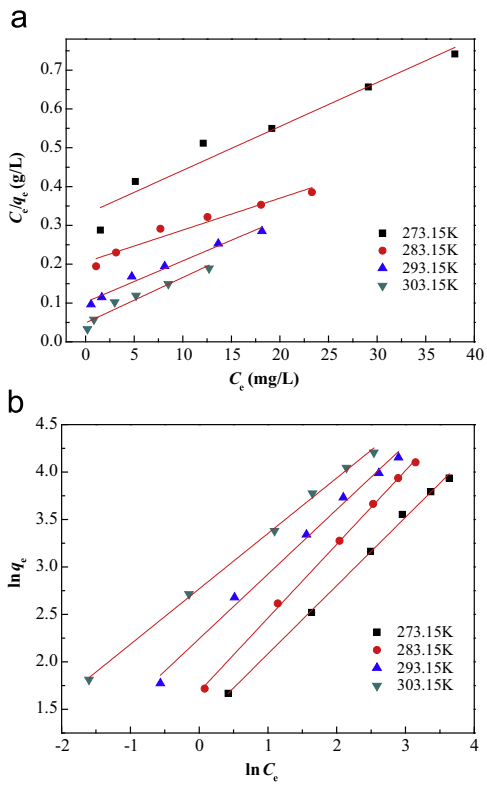

Fig. 7. Linear isotherm plots for the adsorption of ST on PDA@SBP at different temperatures: (a) Langmuir and (b) Freundlich isotherms. The lines indicate the linear fits of the isotherm models concerned.

where q_e and q_{max} represent the equilibrium and maximum adsorption amounts (mg/g), respectively. C_e is the equilibrium dye concentration (mg/L), and K_L (mg/L) and K_F (L/mg) represent constants of the Langmuir and Freundlich models, respectively. $1/n$ is known as Freundlich coefficient related to adsorption intensity of the adsorbent.

To predict if the adsorption is favorable or unfavorable with the Langmuir isotherm, a separation constant factor known as the equilibrium parameter (R_L) was commonly defined by

$$R_L = \frac{1}{1 + C_0 \cdot K_L} \tag{11}$$

where C_0 is the initial concentration of ST (mg/L). $R_L = 0$, $0 < R_L < 1$, $R_L = 1$, and $R_L > 1$ indicate that the Langmuir adsorption process is irreversible, favorable, linear, and unfavorable, respectively.

The linear plots of C_e/q_e versus C_e and $\ln q_e$ against $\ln C_e$ are drawn for the Langmuir and the Freundlich models, respectively which are shown in Fig. 7a and b. The constants (K_L, K_F and $1/n$), the correlation coefficients (R^2), the chi-square (χ^2) and the calculated q_{max} for the two isotherm models are calculated and summarized in Table 3. From the figure and also from the values of statistical parameters, i.e., R^2, χ^2 and F, it is evident that Freundlich model describes very well the dye sorption process for the concentration range studied. The magnitude of K_F shows easy uptake of ST from the aqueous solutions. As can be seen that the value of K_F varied from 3.916 to 15.947 with increasing temperature (273.15–303.15 K), indicating that the adsorption is favorable at high temperatures. Researchers have reported that the Freundlich constant $1/n$ usually depends on the strength and nature of the adsorption process and the $1/n$ of a favorable adsorption is smaller than 1 [40]. In the present case, the value of $1/n$ (0.58–0.77) obtained are below one, suggesting that a favorable adsorption of the dye took place on the surface of PDA@SBP. In addition, the values of R_L for the adsorption of ST are in the range of 0.197–0.740, 0.172–0.714, 0.074–0.490 and 0.033–0.294 at 273.15, 283.15, 293.15 and 303.15 K, respectively. It demonstrates that the ST dye sorption onto PDA@SBP is favorable and therefore the PDA@SBP can be referred as a proper adsorbent for ST adsorption.

Table 3
Adsorption isotherm parameters and thermodynamic parameters for dye adsorption at different temperatures.

T/K	273.15	283.15	293.15	303.15
Langmuir isotherm				
K_L (L/mg)	0.034 ± 0.026	0.040 ± 0.020	0.104 ± 0.013	0.240 ± 0.022
q_{max} (mg/L)	88.417 ± 1.021	121.507 ± 0.351	94.073 ± 2.968	85.470 ± 1.367
R_L	0.197–0.740	0.172–0.714	0.074–0.490	0.033–0.294
R^2	0.939	0.943	0.973	0.938
χ^2	0.127	0.025	0.027	0.015
F	78.701	83.767	188.21	77.281
Freundlich isotherm				
$1/n$	0.719 ± 0.015	0.777 ± 0.011	0.681 ± 0.027	0.584 ± 0.012
K_F (L/mg)	3.916 ± 0.039	5.395 ± 0.025	9.420 ± 0.051	15.947 ± 0.020
R^2	0.997	0.998	0.992	0.997
χ^2	3.770	4.109	4.076	4.157
F	2341.1	4668.6	650.82	2325.4
$-\Delta G^0$ (kJ/mol)	0.410	1.123	2.129	3.033
K_D	1.198	1.612	2.397	3.333
ΔH^0 (kJ/mol)	23.806			
ΔS^0 (J/mol K)	88.473			

3.2.4. Effect of temperature and adsorption thermodynamics

The degree of dye adsorption has been previously identified to be correlated with the temperature of the solid–liquid interface. For investigating the effect of temperature on dye removal process, an analysis of the equilibrium data obtained from isotherm studies held at different temperatures (Fig. 6 and Table 3) is necessary. It is found that the ST dye adsorption capacity presents an apparent increasing tendency while increasing the temperature from 273.15 to 303.15 K, and varies from 51.25 to 67.06 mg/g in initial concentration of 120.0 mg/L. This suggests that the adsorption of ST molecular onto PDA@SBP is favored at higher temperatures within the appropriate temperature range and the adsorption process is endothermic in nature. With the rise in temperature, the rate of diffusion of the adsorbate molecules increases as a result of the decrease of the viscosity of dye solution, resulting in greater adsorption [41,42]. In addition, at higher temperatures, the mobility of dye molecules is significantly enhanced and more ST molecules can interact with the active sites at the surface of PDA@SBP adsorbent particles, thus leading to an increased dye adsorption. An obvious enhancement in adsorption capability was also observed with the rise in temperature for the adsorption of ST onto citric acid modified wheat straw surfaces [43].

In order to describe the feasibility and the inherent energetic changes of adsorption process, the thermodynamic parameters, i.e., the changes in free energy (ΔG^0), entropy (ΔS^0), and enthalpy (ΔH^0) were determined using the Van't Hoff plot by the following formulas:

$$\Delta G^0 = -R \cdot T \cdot \ln K_D \tag{12}$$

$$\ln K_D = \frac{\Delta S^0}{R} - \frac{\Delta H^0}{RT} \tag{13}$$

where R (8.314 J mol^{-1} K^{-1}) is the universal gas constant, T (K) is the absolute temperature. K_D is the distribution coefficient and can

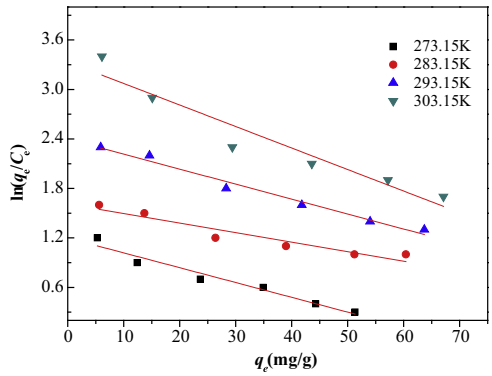

Fig. 8. Plots of ln (q_e/C_e) versus q_e for calculation of thermodynamics.

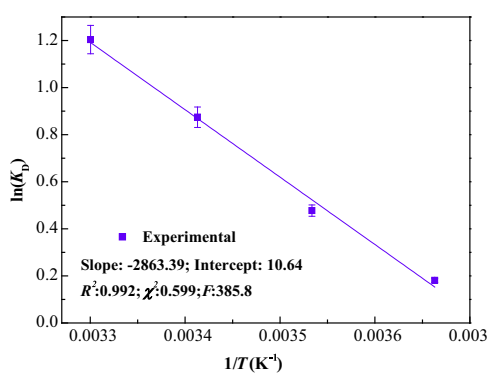

Fig. 9. van't Hoff plot for adsorption of ST onto PDA@SBP.

be calculated from the intercepts of the linear plots of ln (q_e/C_e) versus q_e (Fig. 8). The intercept and slope, respectively of the plots of ln K_D versus $1/T$ gives the values of ΔS^0 and ΔH^0 (Fig. 9).

The calculated negative values of ΔG^0 (−0.410, −1.123, −2.129 and −3.033 kJ/mol at 273.15, 283.15, 293.15 and 303.15 K, respectively) indicate the spontaneity and feasibility of the adsorption [44]. Moreover, the decrease in the negative ΔG^0 value with temperature confirms that a better adsorption is actually obtained at higher temperatures. The magnitude of ΔH^0 was usually employed to classify physisorption and chemisorption, Yao et al. reported that the ΔH^0 of physisorption is smaller than 40 kJ/mol [45]. So the positive value of ΔH^0 (23.806 kJ/mol) suggests that ST adsorption onto PDA@SBP is an endothermic and physisorption process, which is in accordance with the influence of temperature. Meanwhile, the value of ΔS^0 (88.473 J/mol K) was observed to be positive, which illustrates some structure changes in the adsorbent and adsorbate. The positive ΔS^0 also signifies increase in randomness at the solid/solution interface during fixation of ST onto the active sites of PDA@SBP [46]. All the thermodynamic parameters discussed above manifest that PDA@SBP can be used as a high-efficiency adsorbent to remove ST from aqueous solution.

3.2.5. Desorption and reusability

Desorption is a necessary step to analysis the sorption mechanism of PDA@SBP and has a significant and applied value in reuse of the spent adsorbent. Regeneration is an environmentally acceptable option, which may be critical for decreasing process costs and minimizing the waste. For this purpose, it is desirable to desorb the adsorbed ST and regenerate the PDA@SBP for another cycle of adsorption. Here, desorption with distilled water, HCl (0.1 M) and CH_3COOH (0.1 M) was 9.3%, 97.3% and 19.8%, respectively. The low and high desorption of ST by CH_3COOH (0.1 M) and HCl (0.1 M), respectively, manifests that the ST is absorbed onto the adsorbent through physical adsorption [37]. For obtaining the

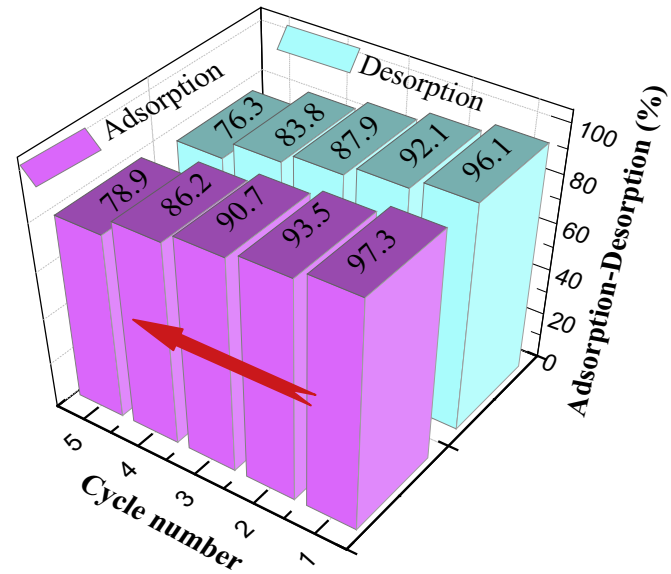

Fig. 10. Adsorption–desorption cycles of ST with 0.1 M HCl as desorbing agent. Conditions: dye concentration: 100.0 mg/L; mass of adsorbent: 50.0 mg; pH: 6.8; temperature: 293.15 K.

versatility of the PDA@SBP, the consecutive adsorption–desorption experiments were conducted with 0.1 M HCl for five cycles (Fig. 10). During five cycles, the adsorption capacity of PDA@SBP was found to be declined from 97.3% to 78.9% and the recovery of ST dye decreased from 96.1% to 76.3%, respectively. So ST molecules could be effectively desorbed, i.e., the PDA@SBP was able to be reused facilely. With increasing number of reuse cycles, the decline of dye-absorbing ability is not so prominent, confirming that the PDA@SBP can be effectively regenerated and successively applied for reuse.

4. Conclusions

In summary, PDA@SBP adsorbent composed of waste seabuckthorn branches coated with a thin layer of polydopamine have been successfully synthesized via a one-pot bio-inspired dip-coating approach. Safranine T, as a typical dye of organic compound used in industry, was chosen to be studied over a batch adsorption system. The experimental results showed that the adsorption process was highly dependent on initial solution pH, initial dye concentration and contact time. The adsorption capacity of ST onto PDA@SBP summed up to 54.0 mg/g at a condition of 100.0 mg/L at 293.15 K, which is much larger than that of neat SBP (17.9 mg/g). Furthermore, the adsorption kinetics and isotherms were found to follow pseudo-second-order kinetic model and Freundlich model, respectively, thermodynamics analysis indicated the ST adsorption was an endothermic, spontaneous, and physisorption process. The change of adsorption capacity after these five repeated cycles of sorption and desorption was marginal which suggests good reusability of the biosorbent. Therefore, the PDA@SBP with simple preparation and practical applicability has combined the high adsorption capacity of pure polydopamine with the low-cost of idle sea buckthorn branch powder substrate, showing great potential as a new class of biosorbent for wastewater treatments.

Acknowledgments

This research was financially supported by Opening Foundation

of Shaanxi Key Laboratory of Exploration and Comprehensive Utilization of Mineral Resources (No. 2014HB001), China Postdoctoral Science Foundation (No. 201104615), and Scientific Research Foundation for the Returned Overseas Chinese Scholars (No. 21176031) and Fundamental Research Funds for the Central Universities (No. 2013G2291015).

References

[1] P. Luo, Y.F. Zhao, B. Zhang, J.D. Liu, Y. Yang, J.F. Liu, Water Res. 44 (2010) 1489–1497.
[2] T. Akar, E. Ozkara, S. Celik, S. Turkyilmaz, S.T. Akar, Colloids Surf. B 101 (2013) 307–314.
[3] J.L. Gong, B. Wang, G.M. Zeng, C.P. Yang, C.G. Niu, Q.Y. Niu, W.J. Zhou, Y. Liang, J. Hazard. Mater. 164 (2009) 1517–1522.
[4] P. Xu, G.M. Zeng, D.L. Huang, C.L. Feng, S. Hu, M.H. Zhao, C. Lai, Z. Wei, C. Huang, G.X. Xie, Z.F. Liu, Sci. Total Environ. 424 (2012) 1–10.
[5] M. Amini, M. Arami, N.M. Mahmmodi, A. Akbari, Desalination 267 (2011) 107–113.
[6] M. Dukkanci, G. Gunduz, S. Yilmaz, R.V. Prihod'ko, J. Hazard. Mater. 181 (2010) 343–350.
[7] J.S. Liu, S. Ma, L.J. Zang, Appl. Surf. Sci. 265 (2013) 393–398.
[8] H. Ma, Q. Zhuo, B. Wang, Chem. Eng. J. 155 (2009) 248–253.
[9] C.-H. Wu, J.-M. Chern, Ind. Eng. Chem. Res. 45 (2006) 6450–6457.
[10] M. Rafatullah, O. Sulaiman, R. Hashim, A. Ahmad, J. Hazard. Mater. 177 (2010) 70–80.
[11] L.L. Qu, T.T. Han, Z.J. Luo, C.C. Liu, Y. Mei, T. Zhu, J. Phys. Chem. Solids 78 (2015) 20–27.
[12] M. Ertas, B. Acemioglu, M.H. Alma, M. Usta, J. Hazard. Mater. 183 (2010) 421–427.
[13] F. Deniz, Environ. Prog. Sustain. (2015) http://dx.doi.org/10.1002/ep.12113.
[14] Y. Premkumar, K. Vijayaraghavan, Sep. Sci. Technol. 9 (2015) 1439–1446.
[15] H.J. Lin, Y. Chen, Tianjin Agric. Sci. 2 (2010) 128–130.
[16] S. Ibrahim, W.Z. Shuy, H.-M. Ang, S. Wang, Asia–Pac. J. Chem. Eng. 5 (2010) 563–569.
[17] H. Lee, S.M. Dellatore, W.M. Miller, P.B. Messersmith, Science 318 (2007) 426–430.
[18] Q. Ye, F. Zhou, W.M. Liu, Chem. Soc. Rev. 40 (2011) 4244–4258.
[19] J.W. Fu, Z.H. Chen, M.H. Wang, S.J. Liu, J.H. Zhang, J.N. Zhang, R.P. Han, Q. Xu, Chem. Eng. J. 259 (2015) 53–61.
[20] N. Farnad, K. Farhadi, N.H. Voelcker, Water Air Soil Pollut. 223 (2012) 3535–3544.
[21] S.H. Yang, S.M. Kang, K.-B. Lee, T.D. Chung, H. Lee, I.S. Choi, J. Am. Chem. Soc. 133 (2011) 2795–2797.
[22] C. Lee, J. Shin, J.S. Lee, E. Byun, J.H. Ryu, S.H. Um, D.-I. Kim, H. Lee, S.W. Cho, Biomacromolecules 14 (2013) 2004–2013.
[23] J.H. Jiang, L.P. Zhu, L.J. Zhu, B.K. Zhu, Y.Y. Xu, Langmuir 27 (2011) 14180–14187.
[24] H. Lee, N.F. Scherer, P.B. Messersmith, Proc. Natl. Acad. Sci. USA 103 (2006) 12999–13003.
[25] L.H. Ai, C.Z. Zhang, F. Liao, Y. Wang, M. Li, L.Y. Meng, J. Jiang, J. Hazard. Mater. 198 (2011) 282–290.
[26] T.S. Anirudhan, A.R. Tharun, S.R. Rejeena, Ind. Eng. Chem. Res. 50 (2011) 1866–1874.
[27] T. Wan, R.Q. Huang, Q.H. Zhao, L. Xiong, L.L. Qin, X.M. Tan, G.J. Cai, J. Appl. Polym. Sci. 130 (2013) 3404–3410.
[28] X.S. Liu, J.M. Cao, H. Li, J.Y. Li, Q. Jin, K.F. Ren, J. Ji, ACS Nano 7 (2013) 9384–9395.
[29] H.O. Ham, Z. Liu, K.H. Lau, H. Lee, P.B. Messersmith, Angew. Chem. Int. Ed. 50 (2011) 732–736.
[30] C. Chao, J.D. Liu, J.T. Wang, Y.W. Zhang, B. Zhang, Y.T. Zhang, X. Xiang, R.F. Chen, ACS Appl. Mater. Interfaces 5 (2013) 10559–10564.
[31] T. Madrakian, A. Afkhami, M. Ahmadi, H. Bagheri, J. Hazard. Mater. 196 (2011) 109–114.
[32] S. Huang, L.P. Yang, M. Liu, S.L. Phua, W.A. Yee, W.S. Liu, R. Zhou, X.H. Lu, Langmuir 29 (2013) 1238–1244.
[33] T.S. Anirudhan, P.S. Suchithra, P. Senan, A.R. Tharun, Ind. Eng. Chem. Res. 51 (2012) 4825–4836.
[34] L.G. Wang, J. Environ. Manag. 102 (2012) 79–87.
[35] M. Ghaedi, F. Karimi, B. Barazesh, R. Sahraei, A. Daneshfar, J. Ind. Eng. Chem. 19 (2013) 756–763.
[36] D.K. Mahmoud, M.A.M. Salleh, W.A.W.A. Karim, A. Idris, Z.Z. Abidin, Chem. Eng. J. 181–182 (2012) 449–457.
[37] I.D. Mall, V.C. Srivastava, G.V.A. Kumar, I.M. Mishra, Colloids Surf. A 278 (2006) 175–187.
[38] Y.N. Patel, M.P. Patel, J. Environ. Chem. Eng. 1 (2013) 1368–1374.
[39] J.Z. Guo, B. Li, L. Liu, K. Lv, Chemosphere 111 (2014) 225–231.
[40] W.S.W. Ngah, S. Fatinathan, J. Environ. Manag. 91 (2010) 958–969.
[41] M. Doğan, H. Abak, M. Alkan, J. Hazard. Mater. 164 (2009) 172–181.
[42] A. Ahmad, M. Rafatullah, O. Sulaiman, M.H. Ibrahima, R. Hashimb, J. Hazard. Mater. 170 (2009) 357–365.
[43] R.P. Han, L.J. Zhang, C. Song, M.M. Zhang, H.M. Zhu, L.J. Zhang, Carbohydr. Polym. 79 (2010) 1140–1149.
[44] M. Auta, B.H. Hameed, Chem. Eng. J. 237 (2014) 350–361.
[45] Y.J. Yao, F.F. Xu, M. Chen, Z.X. Xu, Z.W. Zhu, Bioresour. Technol. 101 (2010) 3040–3046.
[46] R.L. Liu, Y. Liu, X.Y. Zhou, Z.Q. Zhang, J. Zhang, F.Q. Dang, Bioresour. Technol. 154 (2014) 138–147.